Harvesting can stabilize population fluctuations and buffer the impacts of extreme climatic events

Authors

Bart Peeters[1*] (bart.peeters@ntnu.no), Vidar Grøtan[1] (vidar.grotan@ntnu.no), Marlène Gamelon[1,2] (marlene.gamelon@ntnu.no), Vebjørn Veiberg[3] (vebjorn.veiberg@nina.no), Aline M. Lee[1] (lee@alumni.ntnu.no), John M. Fryxell[4] (jfryxell@uoguelph.ca), Steve D. Albon[5] (steve.albon@hutton.ac.uk), Bernt-Erik Sæther[1] (bernt-erik.sather@ntnu.no), Steinar Engen[1] (steinar.engen@ntnu.no), Leif Egil Loe[6] (leif.egil.loe@nmbu.no), Brage Bremset Hansen[1] (brage.b.hansen@ntnu.no)

Affiliations

[1] Centre for Biodiversity Dynamics, Department of Biology, Norwegian University of Science and Technology, NO-7491 Trondheim, Norway.

[2] Laboratoire de Biométrie et Biologie Évolutive, Université Claude Bernard Lyon 1, 69622 Villeurbanne Cedex, France

[3] Norwegian Institute for Nature Research, NO-7485 Trondheim, Norway.

[4] Biodiversity Institute of Ontario, University of Guelph, Guelph, Ontario N1G 2W1, Canada.

[5] The James Hutton Institute, Aberdeen AB15 8QH, UK.

[6] Department of Ecology and Natural Resource Management, Norwegian University of Life Sciences, NO-1432 Ås, Norway.

[*] **Correspondence**: Bart Peeters, NTNU Department of Biology, Høgskoleringen 5, 7491 Trondheim, Norway. E-mail: bart.peeters@ntnu.no

Running title: Harvesting can buffer climate impacts

Keywords: age structure, climate change, demographic modelling, density dependence, exploitation, extreme events, life history, population viability, resource competition, sustainability

Type of article: Letter

Number of words: abstract (150), main text (4862).

Number of references: 55

Number of figures: 5

Authorship statement: B.P., B.B.H. and V.G. designed the study and developed the conceptual ideas with contributions from M.G., V.V., B.-E.S. and J.M.F.; V.G., B.P., A.M.L. and S.E. developed the theoretical models; B.P. and V.G. tested the theoretical models on empirical population data and harvest simulations; B.P. and M.G. performed analyses on the demographic model of Svalbard reindeer with significant contributions of B.B.H., V.G., V.V. and A.M.L.; S.A., L.E.L. and V.V. collected the Svalbard reindeer data; B.P. created visual presentations of the results and wrote the original manuscript; All co-authors reviewed the final manuscript.

Data accessibility statement: The code and data used to produce the results are archived and available on https://doi.org/10.5281/zenodo.5803068.

Competing interests: The authors declare no competing interests.

Abstract

Harvesting can magnify the destabilizing effects of environmental perturbations on population dynamics and, thereby, increase extinction risk. However, population-dynamic theory predicts that impacts of harvesting depend on the type and strength of density-dependent regulation. Here, we used logistic population growth models and an empirical reindeer case study to show that low to moderate harvesting can actually buffer populations against environmental perturbations. This occurs because of density-dependent environmental stochasticity, where negative environmental impacts on vital rates are amplified at high population density due to intraspecific resource competition. Simulations from our population models show that even low levels of harvesting may prevent overabundance, thereby dampening population fluctuations and reducing the risk of population collapse and quasi-extinction following environmental perturbations. Thus, depending on the species' life history and the strength of density-dependent environmental drivers, low to moderate harvesting can improve population resistance to increased climate variability and extreme weather expected under global warming.

Introduction

Overexploitation and climate change represent two of the major anthropogenic threats to biodiversity (Brook *et al.* 2008). While the role of environmental fluctuations in driving population dynamics is now routinely incorporated into models of harvesting and sustainability assessments (Beddington & May 1977; Lande *et al.* 1995; Lande *et al.* 2003), potential interactions between harvesting and climatic drivers are still poorly understood (Gamelon *et al.* 2019). This is alarming, given that climate variability, including the frequency of extreme weather events, have increased due to global warming and are forecasted to intensify further in the near future (Fischer & Knutti 2015; Diffenbaugh *et al.* 2017).

Population-dynamic models generally predict that harvesting can magnify population fluctuations induced by environmental stochasticity and thus increase the risk of extinction (Beddington & May 1977; Lande *et al.* 1995; Lande *et al.* 2003; Hsieh *et al.* 2006; Anderson *et al.* 2008; Fryxell *et al.* 2010; Gamelon *et al.* 2019). This can occur, for instance, due to lagged responses in harvest efforts to population changes (Fryxell *et al.* 2010) or increased environmental sensitivity in age-truncated populations following size-selective harvesting (Hsieh *et al.* 2006; Anderson *et al.* 2008). On the other hand, May and colleagues (May *et al.* 1978) early hypothesized that, in species with chaotic (i.e. irregular) population fluctuations, reducing population density through harvesting can result in less variable population trajectories by dampening the density-dependent effects of environmental stochasticity. Since then, there has been evidence of stabilizing effects of harvesting and 'compensation', i.e., an increase in natural survival and/or recruitment following a reduction in population size due to harvesting or predation, but these depended on the timing of harvesting relative to density-dependent breeding and natural mortality (Boyce *et al.* 1999; Jonzén & Lundberg 1999; Xu *et al.* 2005; Ratikainen *et al.* 2008; Abrams 2009). In cases of overcompensation, harvest or predation mortality have been predicted to lead to even higher population sizes than expected under natural population growth conditions (the so-called "hydra effect", Abrams & Matsuda 2005). However, following May *et al.* (1978), the implications of density-dependent environmental effects have, so far, received little attention in the context of harvesting. This is surprising given the realization that environmental impacts on population dynamics can strongly interact with density (Royama 1992; Coulson *et al.* 2004; Ferguson & Ponciano 2015).

Both theoretical and empirical evidence across taxa now indicate that population dynamics are often characterized by nonlinear amplifications of environmental stochasticity caused by intrinsic processes such as density dependence (Royama 1992; Coulson *et al.* 2001; Barbraud & Weimerskirch 2003; Coulson *et al.* 2004; Stenseth *et al.* 2004; Hsieh *et al.* 2005;

Lima *et al.* 2006; Anderson *et al.* 2008; Ferguson & Ponciano 2015; Gamelon *et al.* 2017; Hansen *et al.* 2019). Interactions between extrinsic (e.g., weather/climate variability) and intrinsic (e.g., density dependence, age structure) mechanisms are particularly expected when competition for food or space is both density-dependent and modulated by environmental conditions (Royama 1992; Owen-Smith 2000; Lima *et al.* 2006). Unfavorable conditions can therefore have multiplicative effects on individual fitness at high density, but little effect at low density (Fig. 1a). Because of this, observed population growth rates of natural populations have sometimes been better explained by density-dependent environmental variance, i.e., multiplicative rather than additive effects of density and climate (Royama 1992; Ferguson & Ponciano 2015; Gamelon *et al.* 2017; Hansen *et al.* 2019). Such 'climate-density interactions' may cause unstable dynamics and population crashes when prolonged periods of favorable conditions lead to high density and high proportions of vulnerable age classes (Festa-Bianchet *et al.* 2003), causing amplified demographic responses to environmental perturbations, such as extreme weather events (Wilmers *et al.* 2007; Ferguson & Ponciano 2015; Hansen *et al.* 2019). Intuitively, strong climate-density interactions would predict that harvesting – which, by definition, reduces density – can weaken the impacts of a subsequent environmental perturbation with density-dependent effects on population dynamics.

Here, we address this prediction using simulations from theoretical population models and an empirically parameterized, stochastic model of demographic rates in wild Svalbard reindeer (*Rangifer tarandus platyrhynchus*). These simulations show that harvesting can weaken the effects of climate-density interaction, leading to increased population stability and resistance to environmental perturbations.

Materials and Methods

Theoretical models

Model properties

To evaluate consequences of harvesting on populations with density-dependent vs. density-independent effects of environmental stochasticity, we considered two discrete time logistic models commonly used in population ecology: the Ricker model and Beverton-Holt model (May *et al.* 1978). Their deterministic analogues can be written as

$$N_{t+1} = N_t e^{\beta_0 - \beta_1 N_t}, \quad [1]$$

for the Ricker model, and

$$N_{t+1} = N_t \frac{e^{\beta_0}}{1 + \beta_1 N_t}, \quad [2]$$

for the Beverton-Holt. In both models, N_t is the population size at time t, e^{β_0} is the maximum population growth rate, and $\beta_1 > 0$ describes the strength of density-dependence in the population growth. The carrying capacity K, i.e., the equilibrium population size, is defined by β_0/β_1 for the Ricker model, and $(e^{\beta_0} - 1)/\beta_1$ for the Beverton-Holt model. The fundamental difference is that, when $N_t \gg K$, the Ricker model produces small N_{t+1} due to strong density dependence, whereas the Beverton-Holt model produces N_{t+1} close to e^{β_0}/β_1 and is, therefore, not characterized by population crashes (de Valpine & Hastings 2002). Furthermore, Ricker dynamics with high values of β_0 lead to overcompensating density dependence, i.e., for N_t near K, decreasing values of $N_t < K$ result in exceedingly higher values of $N_{t+1} > K$. This has been described by the hydra effect in the presence of harvesting or predation (Abrams & Matsuda 2005).

The natural-logarithm transformed version of these models is convenient for parameterizing changes in population size (e.g., de Valpine & Hastings 2002). Let the logistic population growth rate be defined as

$$r_t = \ln(N_{t+1}) - \ln(N_t) = \beta_0 - g(N_t), \quad [3]$$

so that

$$g(N_t) = \beta_1 N_t, \quad [4]$$

for the Ricker model, and

$$g(N_t) = \ln(1 + \beta_1 N_t), \quad [5]$$

for the Beverton-Holt model.

Environmental stochasticity is typically modelled by adding temporal noise on the maximum growth rate, β_0, so that the environmental effect on r_t is independent of N_t (de Valpine & Hastings 2002; Lande *et al.* 2003; Ferguson & Ponciano 2015). We modelled additive environmental variance on the population growth rate as

$$r_t = \beta_0 - g(N_t) + \gamma_a Z_{a,t}. \quad [6]$$

The random variable $Z_{a,t}$ follows a normal distribution with mean 0 and variance 1, the scaling parameter $\gamma_a > 0$ describes the strength of the additive environmental noise, and the variance in the population growth rate is a constant defined by γ_a^2.

However, the effect of environmental stochasticity on the population growth rate often depends on the population density N_t (Ferguson & Ponciano 2015). We modelled multiplicative environmental variance, i.e., density-dependent environmental stochasticity, on the population growth rate as

$$r_t = \beta_0 - g(N_t) e^{-\gamma_m Z_{m,t}}. \quad [7]$$

Similar to $Z_{a,t}$ and γ_a in Eq. 6, the random variable $Z_{m,t}$ follows a normal distribution with mean 0 and variance 1, and the scaling parameter $\gamma_m > 0$ describes the strength of the multiplicative environmental noise. The negative sign of the stochastic term ensures that negative values of $Z_{m,t}$ decrease r_t due to stronger density-dependent environmental variance. In this case, the variance in the population growth rate depends on N_t:

$$\mathrm{Var}[r_t | N_t] = g(N_t)^2 e^{\gamma_m^2} \left(e^{\gamma_m^2} - 1\right). \quad [8]$$

We primarily investigated models with either additive (Eq. 6) or multiplicative (Eq. 7) environmental variance. However, population growth rates can be modelled with both types of environmental variance and covarying $Z_{a,t}$ and $Z_{m,t}$ shaped by a correlation coefficient ρ_Z:

$$r_t = \beta_0 - g(N_t)e^{-\gamma_m Z_{m,t}} + \gamma_a Z_{a,t}\,, \quad [9]$$

$$\mathrm{Var}[r_t|N_t] = \gamma_a^2 + g(N_t)^2 e^{\gamma_m^2}\left(\mathrm{e}^{\gamma_\mathrm{m}^2} - 1\right) - 2g(N_t)\rho_Z\gamma_\mathrm{a}\gamma_m e^{\frac{\gamma_m^2}{2}}. \quad [10]$$

For a given environmental noise $Z_{a,t}$ and $Z_{m,t}$ at time t, the population size $\widehat{N_t}$ that gives $r_t = 0$, sometimes referred to as the stochastic or seasonal carrying capacity K_t (Lande *et al.* 2003; Xu *et al.* 2005), can be expressed as

$$\widehat{N_t} = \frac{\beta_0 + \gamma_a Z_{a,t}}{\beta_1 e^{-\gamma_m Z_{m,t}}}, \quad [11]$$

for the Ricker model, and

$$\widehat{N_t} = \frac{e^{\frac{\beta_0 + \gamma_a Z_{a,t}}{e^{-\gamma_m Z_{m,t}}}} - 1}{\beta_1}, \quad [12]$$

for the Beverton-Holt model.

Model validation

We validated the Ricker and Beverton-Holt models on population growth rates of six ungulate species: ibex (*Capra ibex*, Mignatti *et al.* 2012), Soay sheep (*Ovis aries*, Coulson *et al.* 2001), red deer (*Cervus elaphus*, Bonardi *et al.* 2017), Svalbard reindeer (Hansen *et al.* 2019), mule deer (*Odocoileus hemionus*, Monteith *et al.* 2014), and muskox (*Ovibos moschatus*, Asbjørnsen *et al.* 2005). We selected these population time series as they have previously been shown or suggested to experience density-dependent effects of climatic drivers (Table S1). We first fitted models of observed logistic growth rates with Ricker or Beverton-Holt models and additive (Eq. 6), multiplicative (Eq. 7), or both (Eq. 9) types of environmental variance. We then also analyzed growth rate models with the reported climate variable as an additive or multiplicative

covariate after standardization. Because models with residuals from both additive and multiplicative environmental variance required two extra parameters (i.e., two noise terms and their correlation, Eq. 9-10), we only considered models with either additive or multiplicative residual variance when including the climate covariate. Models were developed with the R-package TMB (Kristensen *et al.* 2016) using the nlminb optimization function to allow the estimation of $Z_{a,t}$ and $Z_{m,t}$ as random effects and minimize the log likelihood between the observed and predicted population growth rate. Model selection was performed using the corrected Akaike's Information Criterion (*AICc*).

Harvest simulations

We investigated consequences of harvesting on population growth rates with additive vs. multiplicative environmental variance. For simplicity, we considered only proportional harvesting for the theoretical models (see 'Reindeer as a case study' below for simulations of constant yield harvesting). Proportional harvesting of magnitude $(1-p)$ was applied to population density at the beginning of each time interval:

$$h(N_t) = N_t(1-p), \quad [13]$$

Density-dependent processes and environmental stochasticity were then applied to the post-harvest population:

$$r_t = \ln\left(h(N_t)e^{\beta_0 - g\left(h(N_t)\right)}\right) - \ln(N_t)\,. \quad [14]$$

This formulation is realistic for many species, such as most Holarctic ungulates, where harvest happens in autumn, mortality rates are highest during winter, and recruitment occurs as birth pulses in spring.

We simulated populations trajectories of 1,000 timesteps for different sets of parameters. Note that the variance in r_t depended on N_t for the models with multiplicative environmental variance (Eq. 8). Therefore, to make models with different types of density

dependence and environmental variance more comparable, we optimized γ_m for given sets of β_0 and β_1 so that $\mathrm{Var}[r_t|N_t = K]_{\mathrm{noharvest}}$ (i.e., the variance in r_t for populations at their carrying capacity in the absence of harvesting) equaled γ_a^2 (i.e., the variance in the population growth rate for models with only additive environmental variance). We calculated the risk of quasi-extinction (i.e., increased extinction risk due to demographic stochasticity when the population size is small) as the proportion of 1,000 simulated population trajectories that experienced $N < K/5$ at least once during 1,000 timesteps.

Reindeer as a case-study

Study population

Arctic ungulates, like Svalbard reindeer, can experience dramatic declines in population size when extreme rain-on-snow (ROS) events occur (Miller & Gunn 2003; Hansen *et al.* 2011; Forbes *et al.* 2016). The tundra vegetation becomes encased in ice as rain- and snowmelt-water freezes on the ground (Peeters *et al.* 2019), thus restricting access to food (Albon *et al.* 2017). The strength of ROS effects on the age-specific vital rates depends on the population density at the time of the event, such that a ROS event strongly affects demographic performances at high density (Hansen *et al.* 2019). Recently, Hansen *et al.* (2019) developed an empirically parameterized stochastic population model where this ROS-density interaction was modelled on vital rates for six age-classes of female Svalbard reindeer. From this population model and simulated ROS-scenarios, they found that increased frequency in extreme ROS events could stabilize population dynamics and reduce extinction risk. The study population, situated in central Spitsbergen (78°N, 16°E), is lightly hunted during autumn, and some reindeer have been culled for scientific purposes (Albon *et al.* 2002), resulting in annual offtakes < 5% of the female population. However, potential harvesting effects accounting for this interaction between ROS and density on reindeer population dynamics have so far remained unclear.

239

240 **Demographic population model**

241 We adopted the demographic population model developed by Hansen *et al.* (2019) to simulate
242 effects of harvesting on the reindeer population dynamics, accounting for age-specific, density-
243 dependent effects of ROS (Fig. 1b). In short, annual population size (*N*) and vital rates (i.e.,
244 survival *S* and fecundity *F*) were estimated for six age classes for the period 1994 to 2014 with
245 an integrated population model (IPM) (Lee *et al.* 2015; Bjørkvoll *et al.* 2016). The six age
246 classes consisted of calves (0 years), yearlings (1 year), and adults of 2, 3-8, 9-11, and ≥12-
247 years. Hansen *et al.* (2019) modelled the effects of postharvest population density
248 ($N_{postharvest}$), winter length, and a three-way interaction between age-class, $N_{postharvest}$, and
249 ROS on age-specific survival and fecundity using linear mixed-effects models (Fig. 1b). To
250 ensure that the effect of ROS was strictly negative (or positive) for all values of $N_{postharvest}$,
251 the ROS-density interaction was included using the form $ROS'_t = ROS_t \times e^{k \times N_{postharvest,t}}$,
252 where the constant k was estimated using an optimization function aiming at minimizing
253 Akaike's Information Criterion (AIC). Year was included as a random effect to account for
254 environmental noise not captured by the fixed parameters, and as a fixed effect to correct for a
255 positive trend in population size during the study period. These models were run for a posterior
256 sample of 9,090 estimates of age-class-specific annual survival, fecundity and population sizes
257 from the IPM (see Table S2 in Hansen *et al.* (2019) for model coefficients).

258 In this study, we simulated population trajectories of 100 years using these models of
259 vital rates with the parameter estimates from 1,000 posterior models. The fixed variable year
260 was set to 2014 and the average observed winter length during 1994-2014 was used for the
261 entire trajectory. Importantly, to account for sources of environmental stochasticity due to
262 processes other than covariates included in the model, we incorporated a covariance matrix of
263 the different vital rates for all age classes. From this covariance matrix, we generated 100 new

residuals from a multivariate normal distribution, i.e., one for each year of the simulated trajectory. These vital rate models then allowed us to estimate the population size at time *t+1* from the population size of each age at time *t*, and simulated ROS and harvest levels.

Changes in the number of females were simulated for ages 0-12, while the number of females ≥13 years old were pooled in one (senescent) age class. Vital rates in the IPM were estimated for six age classes, meaning that the numbers of 12 and ≥13-year-old females were simulated from the vital rates of 9-11 and ≥12 years old, respectively. Using a similar approach to Hansen *et al.* (2019), annual survival and fecundity rates were estimated based on the population size after harvesting $N_{postharvest}$ and stochastic simulations of ROS (Fig. 1b; see "climate-harvesting scenarios" below). Summer mortality for all age classes is considered to be close to zero due to virtual lack of predation (Reimers 1983). The number of individuals of age *j* in year *t* surviving to age *j*+1 was modelled using a binomial process with probability $S_{j,t}$ and n = $N_{j,t}$ random draws to allow for demographic stochasticity (i.e., chance events that affect individuals independently). Similarly, the number of calves born in year *t+1* from the surviving individuals, now age *j+1*, was modelled using a binomial process with probability $F_{j,t}$ and n = $N_{j+1,t+1}$ random draws. Svalbard reindeer do not reach maturity before their second year of life, thus fecundity of calves $F_{0,t}$ = 0, and produce maximum one calf per year (Nowosad 1973). Assuming a balanced sex-ratio (0.5), the total number of female calves was again modelled using a binomial process. The total population size in year *t+1* was then simply calculated by taking the sum of the modelled number of individuals over all ages.

Population trajectories were initiated using the age distribution and population size in year 2014 (N_0 = 1,747; i.e., the last published population estimate from the IPM) (Bjørkvoll *et al.* 2016). Since the IPM estimated population sizes for the six age classes, we estimated the number of females in 2014 for ages 3-12, and ≥13 years, using simple cohort analysis (Solberg *et al.* 1999). This resulted in the following initial age structure from 0 to ≥13 years: 335, 258,

152, 172, 121, 116, 22, 49, 69, 122, 109, 114, 23, and 85 individuals. Nevertheless, the outcome of the 100-year-long trajectories was insensitive to the original age structure.

Climate-harvesting scenarios

We simulated population trajectories for different harvest intensities and three climate scenarios: low, medium, and high frequencies of extreme ROS events (note that these correspond to the very low, medium, and very high frequency scenarios in Hansen *et al.* (2019)). The medium climate scenario reflects the historical state between 1962 and 2014, and simulated realizations of ROS in all three climate scenarios fell within the range of observed values of ROS during this period (see Hansen *et al.* (2019) for further details).

We compared the effects of proportional vs. constant yield harvesting on reindeer population dynamics. A proportional harvest strategy involves a constant effort where, each year, a fixed proportion of the population is harvested (Beddington & May 1977; Lande *et al.* 1995). With a constant harvesting strategy, the same number of individuals are harvested each year. We used fixed harvest proportions ranging from 0 to 0.3 and constant yields of 0 to 300 individuals per year. For simplicity, annual harvest yields were evenly distributed across age classes, i.e., simulating the same age distribution in the harvest offtake as in the pre-harvest population. This is a rather realistic simplification as it reflects the overall management aim to 'shoot through' the population (Peeters *et al.* 2021). For each climate scenario and fixed harvest proportion or constant, we simulated 100-year-long population trajectories based on 10 simulated ROS trajectories for each parameter set of 1,000 posterior models of S and F, i.e., 10,000 population simulations. These were used to calculate population properties, such as average population size, variability in the *per capita* growth rate, and probabilities of a population crash and quasi-extinction. We defined the probability of a population crash within 100 years as a reduction of the pre-harvest population size by half from one year to the next.

The probability of a quasi-extinction within 100 years we defined as a reduction below 20% of the initial population size (N_0 = 1,747, so $N_{\text{quasi-extinct}} < 350$). All analyses were performed using the statistical software R (R Core Team 2019).

Results

Theoretical models

Population time series data of six wild ungulate species clearly demonstrated nonlinear responses to resource-limiting climate variables, with stronger effects at high population density (Fig. 2; see model selection in Table S2 and parameter estimates in Table S3). The form of density dependence was only of significance for Soay sheep, which showed stronger support for Ricker than Beverton-Holt types of growth rates. When no climate covariate was included, models performed clearly better with multiplicative environmental variance, except for muskoxen, which tended to show stronger support for a model with additive environmental variance than a model with both additive and multiplicative variance. Nevertheless, model fitting improved with climate covariates included as a multiplicative term, i.e., interacting with β_1 and N_t. Only for mule deer, a model with an additive climate effect performed marginally better (Table S2), yet with much stronger uncertainty in the estimation of β_0 and β_1 than when the climate covariate was included as a multiplicative term (Table S3).

Both Ricker and Beverton-Holt models with only additive environmental variance showed that increasing harvest proportions increased the variance in (log-)population size (Fig. 3). However, the opposite result was found for models with multiplicative environmental variance, i.e., proportional harvesting reduced the variance in population growth rates (Fig. 4a), leading to stabilized population fluctuations (Figs. 3, 4b) and reduced quasi-extinction risk (Fig. 4c). Particularly for the Ricker model, 'moderate' harvest proportions relative to β_0

buffered population crashes when poor environmental conditions with multiplicative effects occurred at high population density.

Population dynamics from the Beverton-Holt model were not as strongly characterized by population crashes and compensatory dynamics as from the Ricker model, but nevertheless showed that population declines were buffered by harvesting when environmental stochasticity was multiplicative rather than additive to density-dependent population growth (Figs. S1-3). The clearest difference between the Ricker and Beverton-Holt model was the effect of harvesting on the average population size for different maximum growth rates. Ricker dynamics with high values of β_0 displayed compensation of harvesting, i.e., increased average population size, but average population size decreased with harvesting for low values of β_0 and for population trajectories with Beverton-Holt dynamics regardless of β_0 (Fig. 3). However, this was caused by the formulation of density dependence *per se* (Eqs. 4 and 5) and not by how environmental stochasticity entered the models.

Reindeer as a case-study

Simulated population trajectories from our demographic model of Svalbard reindeer (Fig. 1b) showed stabilizing effects of both proportional and constant harvesting on climate-driven fluctuations in population size and age structure (Figs. 5a-c, S4). The risk of population crashes and, consequently, quasi-extinction was highest in the climate scenario with medium (i.e., historical) frequency of ROS events (cf. Hansen *et al.* 2019) but was in all ROS scenarios strongly reduced by annually harvesting a low proportion (< 0.10) of the population (Figs. 5d-e, S4). Moreover, the variance in both population growth rate and log-population size decreased markedly for low to moderate harvest proportions (up to ca. 0.13 and 0.16 for high and low ROS frequencies, respectively Fig. S4). However, the long-run average population size remained approximately unchanged up to these levels of harvesting.

Similarly, for constant harvesting, the variance in population growth rate and log-population size decreased with low to moderate yields (up to ca. 150 and 250 individuals for high and low ROS frequencies, respectively). Constant harvesting reduced the quasi-extinction risk at low harvest yields but not as strongly as comparable levels of proportional harvesting. Also, critical harvest yields, i.e., beyond which the mean population size dropped and quasi-extinction risk sharply increased, varied little between ROS scenarios for proportional harvesting, but strongly for constant harvesting.

Discussion

In this study, we have shown how harvesting can weaken effects of density-dependent environmental stochasticity, leading to stabilized population fluctuations and lower quasi-extinction risks. Depending on the timing of harvesting, this can be expected for systems where bad weather conditions restrict the access to resources and, thereby, increase resource competition nonlinearly with increased population density (Fig. 1) (Royama 1992). Population analyses of six ungulate species (Fig. 2), together with previous findings in the literature (e.g., Coulson *et al.* 2001; Barbraud & Weimerskirch 2003; Ferguson & Ponciano 2015; Gamelon *et al.* 2017), indicated that such climate-density interactions are more common than previously acknowledged, i.e., high population density generally amplified negative effects of overwintering climatic conditions on population growth rates. Both Ricker and Beverton-Holt models with such multiplicative environmental variance revealed stabilizing effects of proportional harvesting on population fluctuations as harvesting reduced the density-dependent effects of environmental stochasticity on the logistic growth rate (Figs. 3-4). Simulations from an age-structured, stochastic model of demographic rates in Svalbard reindeer provided empirically based support for these theoretical findings; low to moderate levels of both proportional and constant yield harvesting can stabilize population dynamics by mitigating

388 climate-density interactions and, thereby, the risk of climate-induced population crashes (Fig.
389 5).

390 In accordance with previous studies (Beddington & May 1977; Lande *et al.* 1995;
391 Lande *et al.* 2003), we found that harvesting increased the variance in log-population size for
392 our theoretical models with only additive environmental variance, making populations more
393 vulnerable to extinction. In contrast, when environmental stochasticity was density-dependent
394 low to moderate harvest proportions reduced the temporal variation in population size and,
395 hence, the probability of quasi-extinction. This occurred because harvesting reduced
396 population density and, thereby, the effects of subsequent density-dependent environmental
397 stochasticity in population growth rates. The reduction in quasi-extinction risk by harvesting
398 thus depends on the relative contributions of density-dependent vs. density-independent
399 environmental variation, and their correlation, as well as the harvest level and maximum
400 population growth rate (Figs. S5-6).

401 In the real world, the demographic responses of natural populations to intrinsic and
402 extrinsic drivers (including harvesting), and their interactions, often depend on their age or
403 stage structure (Caswell 2001; Coulson *et al.* 2001; Festa-Bianchet *et al.* 2003; Lande *et al.*
404 2003). Furthermore, the effects of weather, density and harvesting depend on the timing of
405 harvesting as well as seasonal variation in density-dependent processes and environmental
406 drivers of population dynamics (Boyce *et al.* 1999; Jonzén & Lundberg 1999; Xu *et al.* 2005).
407 The empirically parameterized, stochastic population model for wild Svalbard reindeer (Lee *et*
408 *al.* 2015; Bjørkvoll *et al.* 2016; Hansen *et al.* 2019) provided a heuristic framework to
409 investigate how harvesting can influence population dynamics by modifying density-
410 dependent effects of climatic conditions. Hansen *et al.* (2019) showed how more frequent
411 extreme ROS events reduced the quasi-extinction risk as populations become less likely to

412 exceed their carrying capacity. Overabundant populations are at high risk of collapsing when
413 extreme climate events restrict the *per capita* resource availability.

414 As expected from our theoretical models, we found that harvesting dampened the
415 temporal variation in population growth rates and reduced fluctuations in reindeer abundance
416 and age structure. This happened because harvesting weakened the negative, density-dependent
417 effect of stochastic ROS events on vital rates by decreasing the population density before the
418 onset of winter. Consequently, harvesting reduced the probability of a population crash and,
419 therefore, the risk of climate-induced quasi-extinctions. This empirically based analysis thus
420 confirmed our prediction that, under strong climate-density interactions, harvesting can
421 stabilize population dynamics by buffering negative, density-dependent effects of weather
422 conditions (May *et al.* 1978). While these impacts on stability were already evident at very low
423 harvest proportions (< 0.05), the effects on the long-term average population size were
424 negligible up to a harvest proportion of ca. 0.15 (Fig. S4). Unsurprisingly, increasing harvest
425 proportions further, notably beyond 0.20, increased the risk of quasi-extinction as populations
426 take longer to recover from environmental disturbances and harvest mortality (Beddington &
427 May 1977; Lande *et al.* 1995).

428 In practice, managers often implement a quota harvesting strategy. Proportional,
429 threshold and proportional threshold harvesting are generally recommended as more
430 sustainable harvest strategies, but these require estimates of abundance which typically are
431 unavailable or come with large uncertainties (Lande *et al.* 1995; Engen *et al.* 1997).
432 Interestingly, though, low constant harvest yields in our reindeer model also reduced
433 population fluctuations without affecting the long-term average population size. Nevertheless,
434 the stabilizing effect and reduction in quasi-extinction risk were less prominent than for harvest
435 proportions with similar impacts. Also, the critical constant harvest yield beyond which the
436 quasi-extinction risk increased steeply was very sensitive to the frequency of ROS events (Fig.

S4), indicating that constant harvesting is a less sustainable strategy for populations subject to such climate change.

The combined results from simulations and realistic population models suggest that harvesting can indeed increase population stability and resistance to environmental perturbations (May *et al.* 1978). This has important general implications far beyond our case-study system. Previous studies across vertebrate species (Royama 1992; Owen-Smith 2000; Coulson *et al.* 2001; Barbraud & Weimerskirch 2003; Coulson *et al.* 2004; Stenseth *et al.* 2004; Lima *et al.* 2006; Ferguson & Ponciano 2015; Gamelon *et al.* 2017; Hansen *et al.* 2019) as well as our comparative analysis in six ungulate species (Fig. 3) clearly indicate that, in seasonal, resource-limited systems, climate-density interactions in population dynamics are far more common than previously acknowledged. Therefore, harvesting will often modify the effects of density-dependent environmental stochasticity on population dynamics. By avoiding overabundant populations, managers could even buffer population crashes induced by stochastic extreme events that affect individual fitness through resource competition. Accordingly, sustainable levels of harvesting can serve as a management (and even conservation) strategy to weaken negative effects of increased climate variability and extreme events (e.g., flooding, drought, storms) anticipated under global climate change (Fischer & Knutti 2015; Diffenbaugh *et al.* 2017). The sustainability of implementing harvesting as a strategy to stabilize population dynamics and avoid population crashes will, however, depend on, e.g., the strength of density-dependent vs. density-independent environmental effects, the implemented harvest strategy, and the frequency and magnitude of stochastic climate perturbations.

Thus, the stabilizing effect of harvesting outlined here will not apply to all species or under all circumstances. For one thing, population resistance to environmental perturbations and implications of harvesting depend on the species' life history strategy. Moreover, density-

462 independent stochastic mechanisms (May *et al.* 1978; Lande *et al.* 2003), as well as ecological
463 and evolutionary consequences of selective harvesting (Anderson *et al.* 2008; Pigeon *et al.*
464 2016; Leclerc *et al.* 2017), can make populations more sensitive to temporal variation in the
465 environment (Gamelon *et al.* 2019). Population resistance to environmental perturbations also
466 depends on the harvesting strategy (Beddington & May 1977; Lande *et al.* 1995) and
467 stochasticity in harvesting processes (Jonzén *et al.* 2002), sometimes causing lagged responses
468 in effort and quota regulations to resource fluctuations (Fryxell *et al.* 2010). Autocorrelation
469 and seasonal variation in the strengths of density-dependent vs. density-independent
470 environmental variance may also complicate the stabilizing effects of harvesting. Nevertheless,
471 our discrete-time logistic models are approximate for systems, such as many ungulate
472 populations, where harvesting reduces population density just before natural population
473 changes are driven by density dependence and environmental stochasticity. Stabilizing effects
474 of harvesting under climate-density interactions likely occur in resource-limited systems with
475 strong compensatory responses among survivors of harvesting (Boyce *et al.* 1999; Jonzén &
476 Lundberg 1999). Such buffering effects of harvesting could explain why climate-density
477 interactions seem to be more evident in populations with no (or very low) harvesting than in
478 heavily harvested populations (Tveraa *et al.* 2007). Thus, our study highlights that, especially
479 in the context of global warming, the future sustainability of wildlife resource exploitation
480 requires a better understanding of the potential interactions of climate, internal population
481 regulation, and harvesting strategies.
482
483 **Acknowledgements:** We thank our collaborators and field assistants from the Svalbard
484 reindeer study system. We also thank Mark Boyce and one anonymous reviewer whose
485 feedback greatly improved the quality of our results. The reindeer picture was provided with
486 permission for publication by Larissa T. Beumer. **Funding**: This study was funded by the

Norwegian Research Council through projects 223257 (Centres of Excellence funding scheme), 244647 (KLIMAFORSK) and 276080 (FRIMEDBIO), and the Centre for Biodiversity Dynamics at the Norwegian University of Science and Technology.

References

1.
Abrams, P.A. (2009). When does greater mortality increase population size? The long history and diverse mechanisms underlying the hydra effect. *Ecol. Lett.*, 12, 462-474.
2.
Abrams, P.A. & Matsuda, H. (2005). The effect of adaptive change in the prey on the dynamics of an exploited predator population. *Can. J. Fish. Aquat. Sci.*, 62, 758-766.
3.
Albon, S.D., Irvine, R.J., Halvorsen, O., Langvatn, R., Loe, L.E., Ropstad, E. *et al.* (2017). Contrasting effects of summer and winter warming on body mass explain population dynamics in a food-limited Arctic herbivore. *Glob. Change Biol.*, 23, 1374-1389.
4.
Albon, S.D., Stien, A., Irvine, R.J., Langvatn, R., Ropstad, E. & Halvorsen, O. (2002). The role of parasites in the dynamics of a reindeer population. *Proc. R. Soc. B*, 269, 1625-1632.
5.
Anderson, C.N.K., Hsieh, C.-H., Sandin, S.A., Hewitt, R., Hollowed, A., Beddington, J. *et al.* (2008). Why fishing magnifies fluctuations in fish abundance. *Nature*, 452, 835-839.
6.
Asbjørnsen, E.J., Sæther, B.-E., Linnell, J.D.C., Engen, S., Andersen, R. & Bretten, T. (2005). Predicting the growth of a small introduced muskox population using population prediction intervals. *J. Anim. Ecol.*, 74, 612-618.
7.
Barbraud, C. & Weimerskirch, H. (2003). Climate and density shape population dynamics of a marine top predator. *Proc. R. Soc. B*, 270, 2111-2116.
8.
Beddington, J.R. & May, R.M. (1977). Harvesting natural populations in a randomly fluctuating environment. *Science*, 197, 463-465.
9.
Bjørkvoll, E., Lee, A.M., Grøtan, V., Sæther, B.E., Stien, A., Engen, S. *et al.* (2016). Demographic buffering of life histories? Implications of the choice of measurement scale. *Ecology*, 97, 40-47.
10.
Bonardi, A., Corlatti, L., Bragalanti, N. & Pedrotti, L. (2017). The role of weather and density dependence on population dynamics of Alpine-dwelling red deer. *Integr. Zool.*, 12, 61-76.
11.
Boyce, M.S., Sinclair, A.R.E. & White, G.C. (1999). Seasonal compensation of predation and harvesting. *Oikos*, 87, 419-426.
12.

531 Brook, B.W., Sodhi, N.S. & Bradshaw, C.J.A. (2008). Synergies among extinction drivers
532 under global change. *Trends in Ecology & Evolution*, 23, 453-460.
533 13.
534 Caswell, H. (2001). *Matrix population models: construction, analysis, and interpretation*.
535 Sinauer Associates, Sunderland, Massachusetts.
536 14.
537 Coulson, T., Catchpole, E.A., Albon, S.D., Morgan, B.J.T., Pemberton, J.M., Clutton-Brock,
538 T.H. *et al.* (2001). Age, sex, density, winter weather, and population crashes in Soay
539 sheep. *Science*, 292, 1528-1531.
540 15.
541 Coulson, T., Rohani, P. & Pascual, M. (2004). Skeletons, noise and population growth: the end
542 of an old debate? *Trends Ecol. Evol.*, 19, 359-364.
543 16.
544 de Valpine, P. & Hastings, A. (2002). Fitting population models incorporating process noise
545 and observation error. *Ecol. Monogr.*, 72, 57-76.
546 17.
547 Diffenbaugh, N.S., Singh, D., Mankin, J.S., Horton, D.E., Swain, D.L., Touma, D. *et al.* (2017).
548 Quantifying the influence of global warming on unprecedented extreme climate events.
549 *PNAS*, 114, 4881-4886.
550 18.
551 Engen, S., Lande, R. & Sæther, B.-E. (1997). Harvesting strategies for fluctuating populations
552 based on uncertain population estimates. *J. Theor. Biol.*, 186, 201-212.
553 19.
554 Ferguson, J.M. & Ponciano, J.M. (2015). Evidence and implications of higher-order scaling in
555 the environmental variation of animal population growth. *PNAS*, 112, 2782-2787.
556 20.
557 Festa-Bianchet, M., Gaillard, J.-M. & Côté, S.D. (2003). Variable age structure and apparent
558 density dependence in survival of adult ungulates. *J. Anim. Ecol.*, 72, 640-649.
559 21.
560 Fischer, E.M. & Knutti, R. (2015). Anthropogenic contribution to global occurrence of heavy-
561 precipitation and high-temperature extremes. *Nat. Clim. Change*, 5, 560-564.
562 22.
563 Forbes, B.C., Kumpula, T., Meschtyb, N., Laptander, R., Macias-Fauria, M., Zetterberg, P. *et*
564 *al.* (2016). Sea ice, rain-on-snow and tundra reindeer nomadism in Arctic Russia. *Biol.*
565 *Lett.*, 12.
566 23.
567 Fryxell, J.M., Packer, C., McCann, K., Solberg, E.J. & Sæther, B.-E. (2010). Resource
568 management cycles and the sustainability of harvested wildlife populations. *Science*,
569 328, 903-906.
570 24.
571 Gamelon, M., Grøtan, V., Nilsson, A.L.K., Engen, S., Hurrell, J.W., Jerstad, K. *et al.* (2017).
572 Interactions between demography and environmental effects are important
573 determinants of population dynamics. *Sci. Adv.*, 3, e1602298.
574 25.
575 Gamelon, M., Sandercock, B.K. & Sæther, B.-E. (2019). Does harvesting amplify
576 environmentally induced population fluctuations over time in marine and terrestrial
577 species? *J. Appl. Ecol.*, 56, 2186– 2194.
578 26.

579 Hansen, B.B., Gamelon, M., Albon, S.D., Lee, A.M., Stien, A., Irvine, R.J. *et al.* (2019). More
580 frequent extreme climate events stabilize reindeer population dynamics. *Nat. Commun.*,
581 10, 1616.
582 27.
583 Hansen, B.B., Aanes, R., Herfindal, I., Kohler, J. & Sæther, B.-E. (2011). Climate, icing, and
584 wild arctic reindeer: past relationships and future prospects. *Ecology*, 92, 1917-1923.
585 28.
586 Hsieh, C.-H., Glaser, S.M., Lucas, A.J. & Sugihara, G. (2005). Distinguishing random
587 environmental fluctuations from ecological catastrophes for the North Pacific Ocean.
588 *Nature*, 435, 336-340.
589 29.
590 Hsieh, C.-H., Reiss, C.S., Hunter, J.R., Beddington, J.R., May, R.M. & Sugihara, G. (2006).
591 Fishing elevates variability in the abundance of exploited species. *Nature*, 443, 859-
592 862.
593 30.
594 Jonzén, N. & Lundberg, P. (1999). Temporally structured density-dependence and population
595 management. *Ann. Zool. Fennici*, 36, 39-44.
596 31.
597 Jonzén, N., Ripa, J. & Lundberg, P. (2002). A theory of stochastic harvesting in stochastic
598 environments. *Am. Nat.*, 159, 427-437.
599 32.
600 Kristensen, K., Nielsen, A., Berg, C.W., Skaug, H. & Bell, B.M. (2016). TMB: Automatic
601 differentiation and Laplace approximation. *J. Stat. Softw.*, 70, 1-21.
602 33.
603 Lande, R., Engen, S. & Sæther, B.-E. (1995). Optimal harvesting of fluctuating populations
604 with a risk of extinction. *Am. Nat.*, 145, 728-745.
605 34.
606 Lande, R., Sæther, B.-E. & Engen, S. (2003). *Stochastic population dynamics in ecology and*
607 *conservation*. Oxford University Press, Oxford.
608 35.
609 Leclerc, M., Zedrosser, A. & Pelletier, F. (2017). Harvesting as a potential selective pressure
610 on behavioural traits. *J. Appl. Ecol.*, 54, 1941-1945.
611 36.
612 Lee, A.M., Bjørkvoll, E.M., Hansen, B.B., Albon, S.D., Stien, A., Sæther, B.-E. *et al.* (2015).
613 An integrated population model for a long-lived ungulate: more efficient data use with
614 Bayesian methods. *Oikos*, 124, 806-816.
615 37.
616 Lima, M., Previtali, M.A. & Meserve, P.L. (2006). Climate and small rodent dynamics in semi-
617 arid Chile: the role of lateral and vertical perturbations and intra-specific processes.
618 *Clim. Res.*, 30, 125-132.
619 38.
620 May, R.M., Beddington, J.R., Horwood, J.W. & Shepherd, J.G. (1978). Exploiting natural
621 populations in an uncertain world. *Math. Biosci.*, 42, 219-252.
622 39.
623 Mignatti, A., Casagrandi, R., Provenzale, A., von Hardenberg, A. & Gatto, M. (2012). Sex-
624 and age-structured models for Alpine ibex *Capra ibex ibex* population dynamics.
625 *Wildlife Biol*, 18, 318-332.
626 40.
627 Miller, F.L. & Gunn, A. (2003). Catastrophic die-off of Peary caribou on the western queen
628 Elizabeth Islands, Canadian High Arctic. *Arctic*, 56, 381-390.

629 41.
630 Monteith, K.L., Bleich, V.C., Stephenson, T.R., Pierce, B.M., Conner, M.M., Kie, J.G. *et al.*
631 (2014). Life-history characteristics of mule deer: effects of nutrition in a variable
632 environment. *Wildl. Monogr.*, 186, 1-62.
633 42.
634 Nowosad, R.F. (1973). Twinning in reindeer. *J. Mammal.*, 54, 781.
635 43.
636 Owen-Smith, N. (2000). Modeling the population dynamics of a subtropical ungulate in a
637 variable environment: Rain, cold and predators. *Nat. Resour. Model.*, 13, 57-87.
638 44.
639 Peeters, B., Pedersen, Å.Ø., Loe, L.E., Isaksen, K., Veiberg, V., Stien, A. *et al.* (2019).
640 Spatiotemporal patterns of rain-on-snow and basal ice in high Arctic Svalbard:
641 detection of a climate-cryosphere regime shift. *Environ. Res. Lett.*, 14, 015002.
642 45.
643 Peeters, B., Pedersen, Å.Ø., Veiberg, V. & Hansen, B.B. (2021). Hunting quotas, selectivity
644 and stochastic population dynamics challenge the management of wild reindeer. *Clim.*
645 *Res.*, SUSTAIN av12.
646 46.
647 Pigeon, G., Festa-Bianchet, M., Coltman, D.W. & Pelletier, F. (2016). Intense selective hunting
648 leads to artificial evolution in horn size. *Evol. Appl.*, 9, 521-530.
649 47.
650 R Core Team (2019). R: A language and environment for statistical computing. R Foundation
651 for Statistical Computing Vienna, Austria.
652 48.
653 Ratikainen, II, Gill, J.A., Gunnarsson, T.G., Sutherland, W.J. & Kokko, H. (2008). When
654 density dependence is not instantaneous: theoretical developments and management
655 implications. *Ecol. Lett.*, 11, 184-198.
656 49.
657 Reimers, E. (1983). Mortality in Svalbard reindeer. *Holarctic Ecol*, 6, 141-149.
658 50.
659 Royama, T. (1992). *Analytical population dynamics*. Chapman & Hall, London.
660 51.
661 Solberg, E.J., Sæther, B.-E., Strand, O. & Loison, A. (1999). Dynamics of a harvested moose
662 population in a variable environment. *J. Anim. Ecol.*, 68, 186-204.
663 52.
664 Stenseth, N.C., Chan, K.S., Tavecchia, G., Coulson, T., Mysterud, A., Clutton-Brock, T. *et al.*
665 (2004). Modelling non-additive and nonlinear signals from climatic noise in ecological
666 time series: Soay sheep as an example. *Proc. R. Soc. B*, 271, 1985-1993.
667 53.
668 Tveraa, T., Fauchald, P., Yoccoz, N.G., Ims, R.A., Aanes, R. & Hogda, K.A. (2007). What
669 regulate and limit reindeer populations in Norway? *Oikos*, 116, 706-715.
670 54.
671 Wilmers, C.C., Post, E. & Hastings, A. (2007). A perfect storm: the combined effects on
672 population fluctuations of autocorrelated environmental noise, age structure, and
673 density dependence. *Am. Nat.*, 169, 673-683.
674 55.
675 Xu, C.L., Boyce, M.S. & Daley, D.J. (2005). Harvesting in seasonal environments. *J. Math.*
676 *Biol.*, 50, 663-682.
677

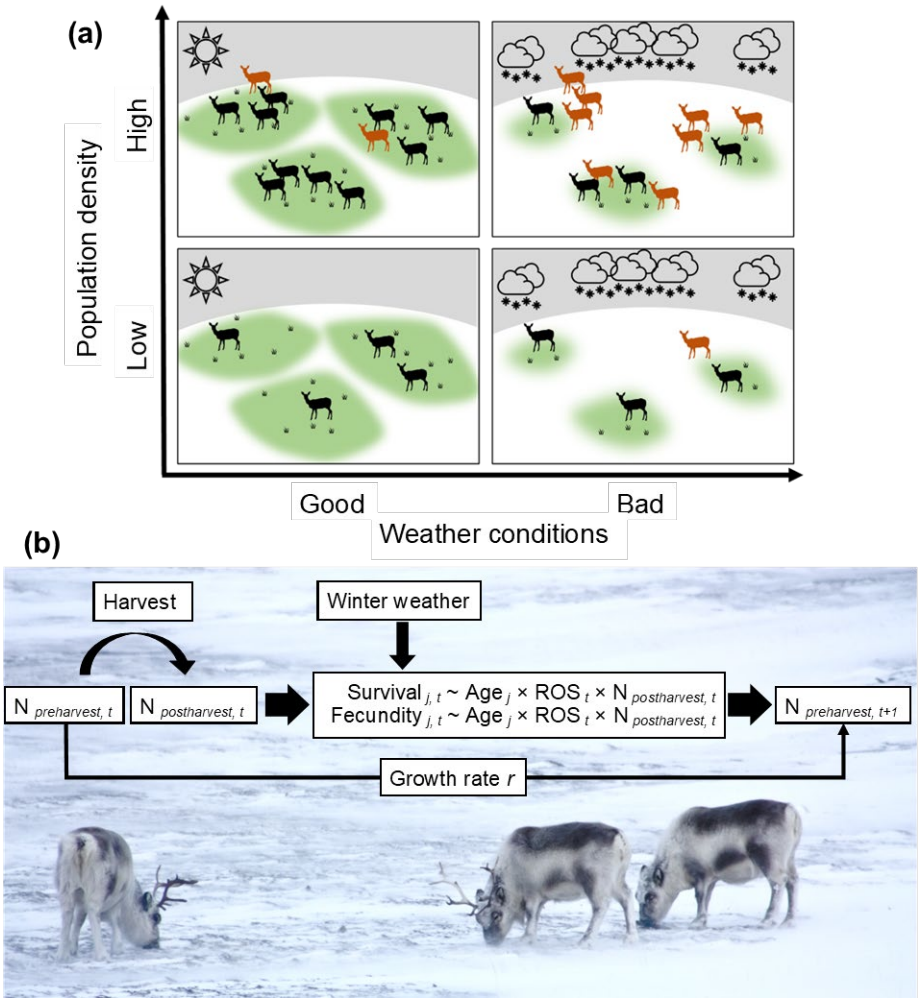

Fig. 1| Conceptual diagram of climate-density interactions and the demographic reindeer model. (a) The *per capita* resource availability is highest when population density is low and weather conditions are good. At high population density and good weather conditions, resource competition becomes more influenced by density-dependent processes, but not weather. However, when bad weather conditions restrict the *per capita* resource availability, the effects of weather on demographic rates (red animals indicate individual mortality) are limited at low population density, but amplified by density-dependent processes at high population density. **(b)** In Svalbard reindeer, bad winters correspond to high amounts of rain-on-snow (ROS), causing snowpack icing and restricted access to winter forage. This leads to stronger effects of ROS on vital rates (Survival, Fecundity) at high population density (N) and for juvenile and old individuals (Age j).

690

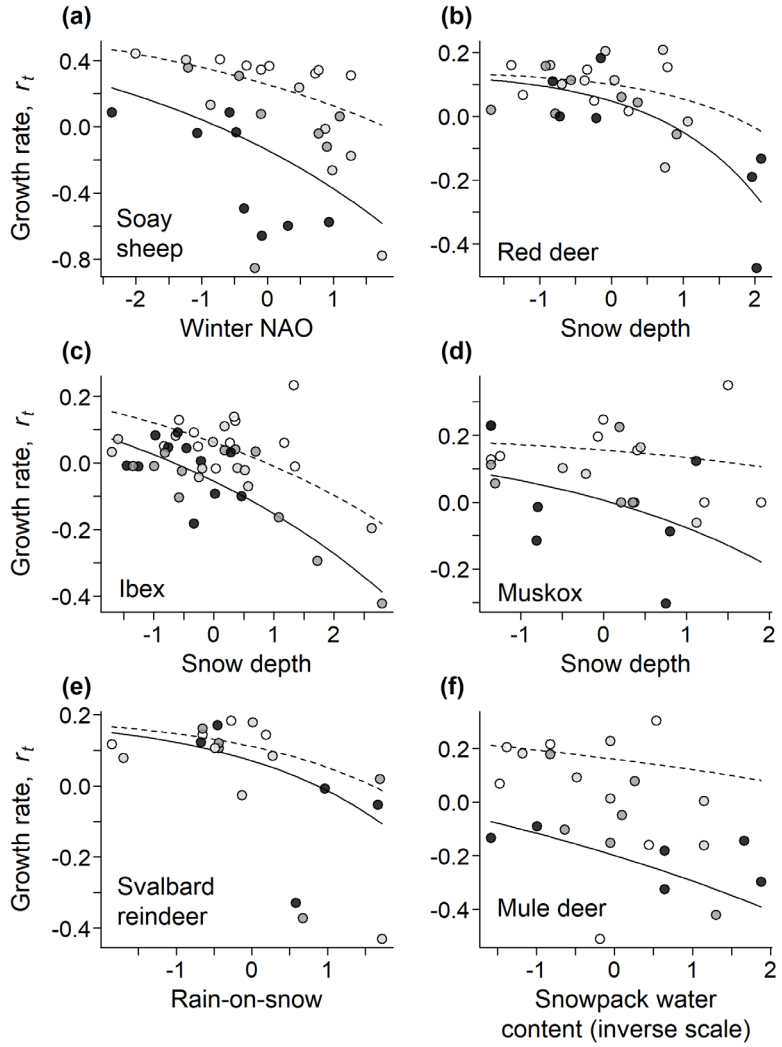

691

692 **Fig. 2| Climate-density interactions in ungulate populations.** Nonlinear, density-dependent
693 effects of weather on population growth rate (r_t) are found in (**a**) Soay sheep, (**b**) red deer, (**c**)
694 ibex, (**d**) muskox, (**e**) Svalbard reindeer, and (**f**) mule deer. Weather variables were
695 standardized. Dot colors indicate low (white), medium (grey), and high (black) observed
696 population sizes. Predicted responses of density-dependent population growth rate are shown
697 for low (mean − 1SD; dashed lines) and high (mean + 1SD; solid lines) population sizes.

698

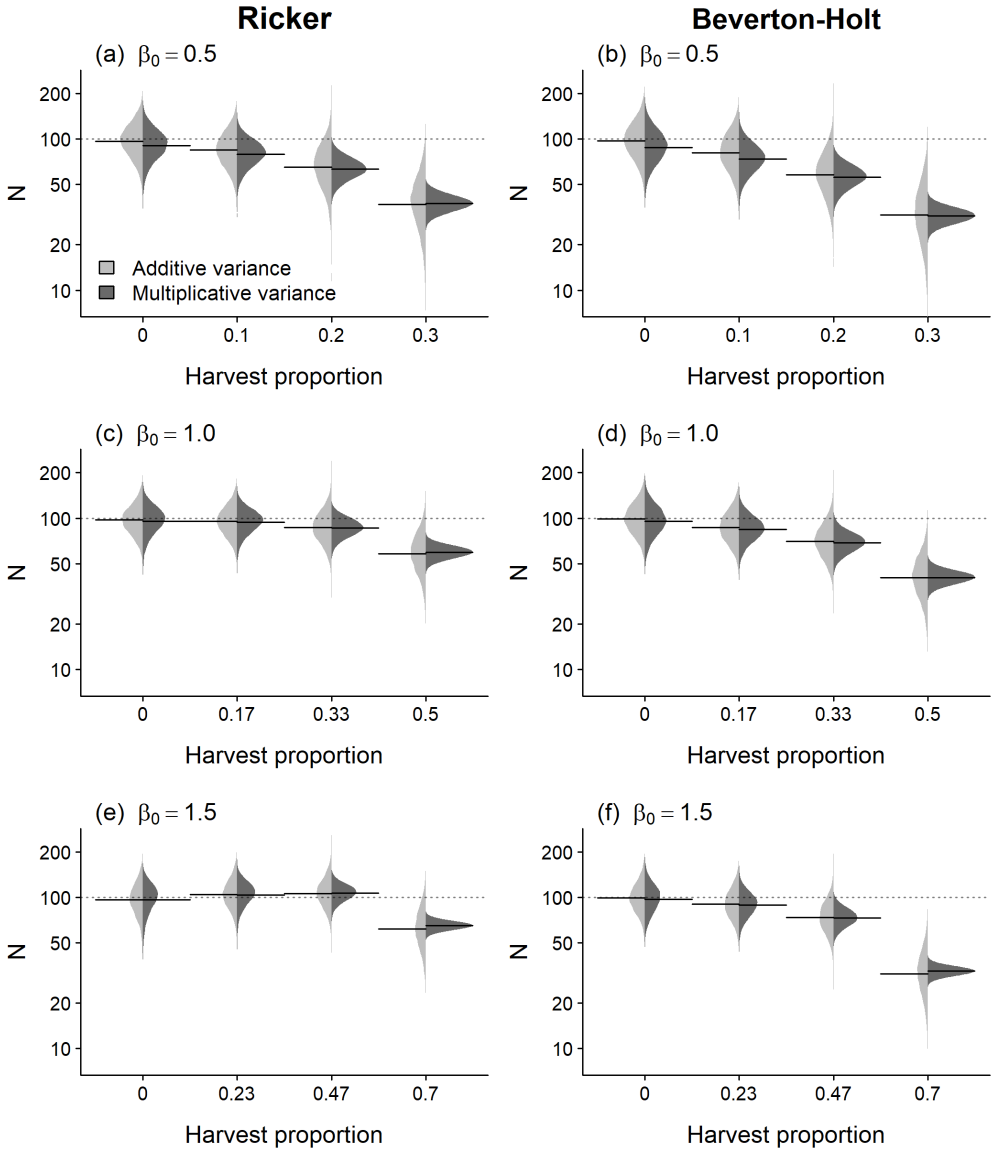

Fig. 3| Effects of proportional harvesting on the distribution of population sizes for Ricker (left panels) and Beverton-Holt (right panels) models with additive (grey distributions) vs. multiplicative (black distributions) environmental variance, and maximum growth rates (**a, b**) β_0 = 0.5, (**c, d**) β_0 = 1.0, and (**e, f**) β_0 = 1.5. Average population sizes are indicated by black horizontal lines. Note that x-axes are on different scales for the different values of β_0 and y-axes are on log-scale. Chosen parameters were K = 100 (grey horizontal lines), γ_a = 0.224, and γ_m the resultant value when the variance of r = 0.05 for $N = K$ in the absence of harvesting (i.e., $\mathrm{Var}[r_t|N_t = K]_{\mathrm{noharvest}}$); (a, b) γ_m = 0.397, (c, d) γ_m = 0.216, (e, f) γ_m = 0.147.

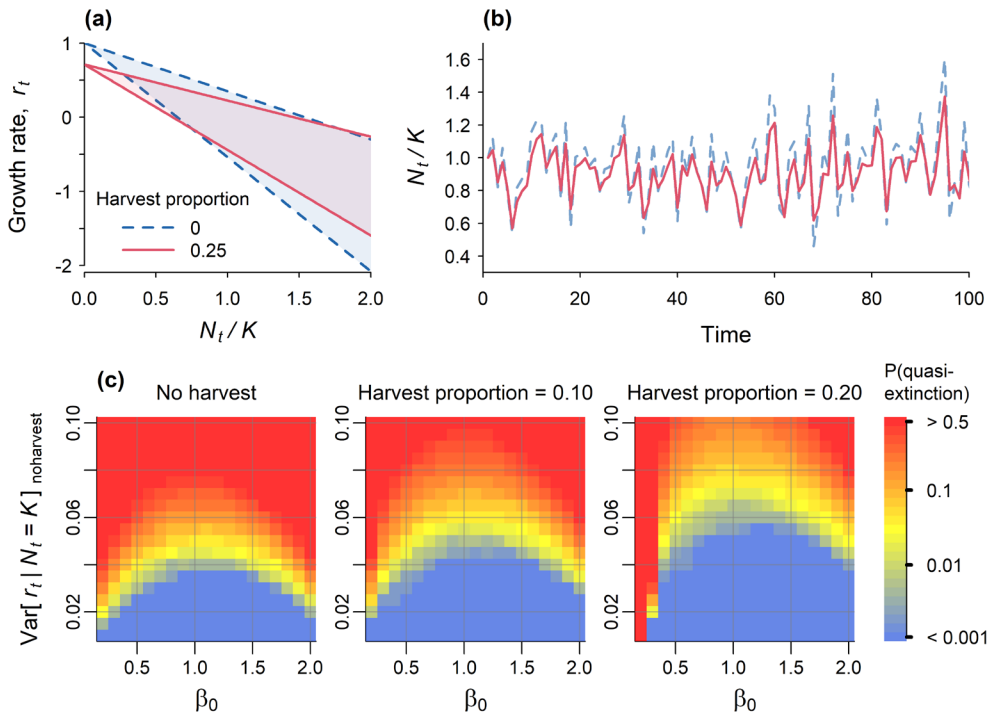

Fig. 4| Proportional harvesting reduces population fluctuations and quasi-extinction risk. Effects of proportional harvesting in the Ricker logistic growth rate model with multiplicative environmental variance. (**a**) Distribution in population growth rate (r_t) as a function of population density (N_t/K) and harvest proportions 0 (blue shade and dashed lines) and 0.25 (red shade and solid lines), and (**b**) simulated population trajectories. Chosen parameters are β_0 = 1.0, K =100, γ_m= 0.22. (**c**) Probabilities of quasi-extinction (increasing $P(N < K/5)$ indicated by the blue-to-red gradient) for increasing harvest proportions (left = 0, center = 0.1, right = 0.2), maximum growth rates (β_0, x-axis), and variance in growth rate (y-axis, shown for populations at their carrying capacity (K) in the absence of harvesting, $\mathrm{Var}[r_t|N_t = K]_{\mathrm{noharvest}}$).

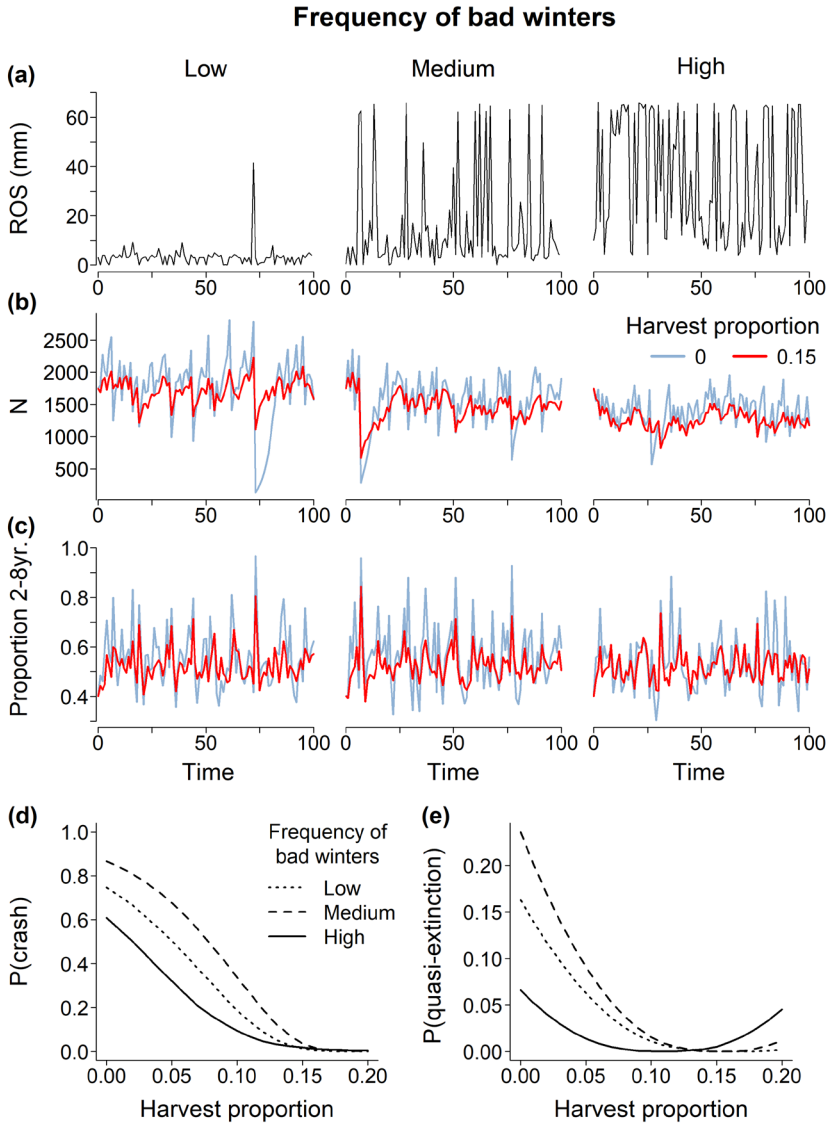

721

722 **Fig. 5| Stabilizing effects of harvesting in a climate-driven population of high Arctic**
723 **reindeer.** (**a**) Simulated trajectories with low to high frequencies of ROS events and
724 consequent responses in (**b**) female population size and (**c**) the proportion of prime-aged (2-8
725 yr. old) females, indicating stabilizing effects of proportional harvesting (red lines = 0.15, blue
726 lines = no harvesting). (**d**) Probability of population crashes and (**e**) probability of quasi-
727 extinction in response to proportional harvesting for low (dotted lines), medium (dashed lines),
728 and high (solid lines) frequencies of bad winters.